

AD-A055 732

PRINCETON UNIV N J DEPT OF CIVIL AND GEOLOGICAL ENG--ETC F/G 20/2  
EDGE DISLOCATION IN NONLOCAL HEXAGONAL ELASTIC CRYSTALS.(U)  
MAY 78 A C ERINGEN, F BALTA

N00014-76-C-0240

UNCLASSIFIED

78-SM-3

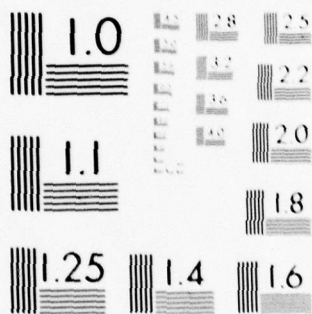
NL

| of |

AD  
A055 732



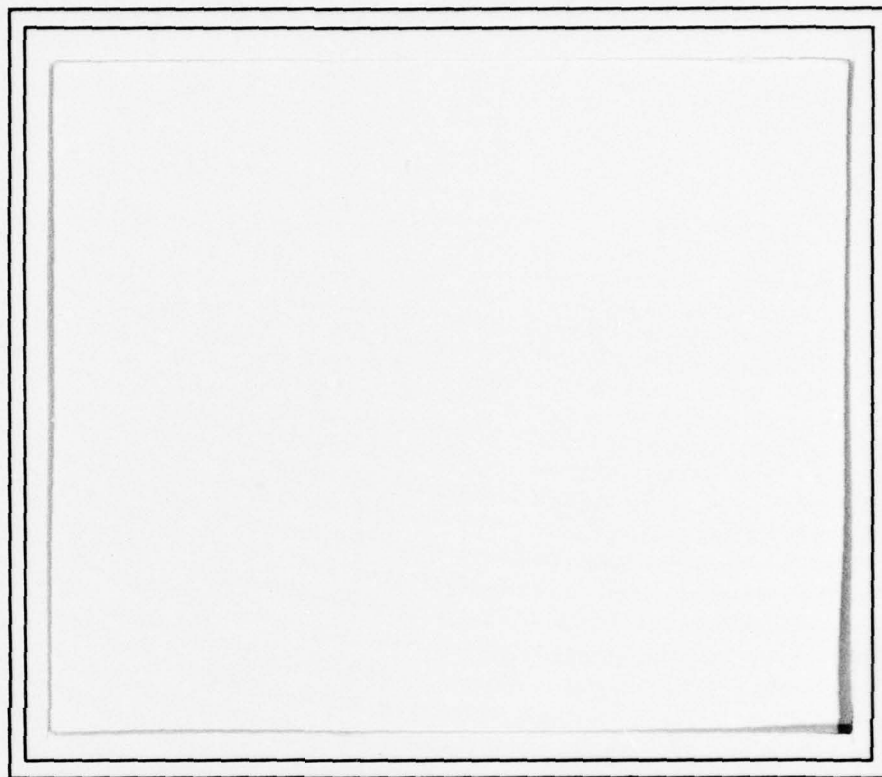
END  
DATE  
FILMED  
8 -78  
DDC



MICROCOPY RESOLUTION TEST CHART

FOR FURTHER TRANSMISSION

12



PRINCETON UNIVERSITY  
*Department of Civil Engineering*



This document has been approved  
for public release and sale; its  
distribution is unlimited.

DDC  
JUN 22 1978  
RECEIVED  
Ely

STRUCTURES AND MECHANICS

78 06 21 004

DDC FILE COPY

AD A055732

Technical Rep. No. ~~52~~ 49 ✓  
Civil Engng. Res. Rep. No. 78-SM-3 ✓

⑥ EDGE DISLOCATION IN NONLOCAL  
HEXAGONAL ELASTIC CRYSTALS.

by

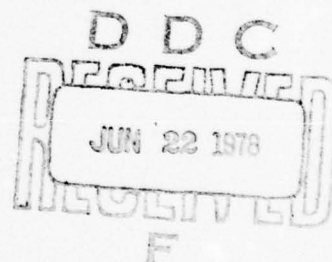
⑨ Technical rept.

⑩ A. Cemal Eringen  
and  
F. Balta

Research Sponsored by the  
Office of Naval Research

⑮ under  
Contract N00014-76-C-0240  
Modification No. P00002

⑭ 78-SM-3, TR-49



⑪ May 1978

⑫ 29p.

Approved for Public Release; Distribution Unlimited

78 06 21 004  
401 272

50B



EDGE DISLOCATION IN NONLOCAL  
HEXAGONAL ELASTIC CRYSTALS\*

by  
A. Cemal Eringen  
and  
F. Balta  
Princeton University

ABSTRACT

The solution is presented for the problems of edge dislocation in hexagonal crystals with long range interatomic interactions. The field equations of nonlocal elastic solids are employed to determine the stress fields and the elastic energy for an edge dislocation in the basal plane. Classical stress and energy singularities are found not present in the nonlocal solutions. Stress distribution is calculated and maximum shear stress is given for various hexagonal materials. Theoretical shear stress to initiate a dislocation having a Burger's vector of one atomic distance is calculated and found to be in the acceptable range known from the lattice dynamic calculations.

1. INTRODUCTION

It is well-known that the classical elasticity solution of the edge dislocation contains stress and energy singularities in the "core region", cf. [1]. In several previous papers (e.g., [2], [3], [4]) we have shown that the solutions of various Volterra dislocations based on the nonlocal elasticity theory do not contain

---

\*The present work was supported by the Office of Naval Research

these singularities. This recent theory [5,6] models the elastic materials much more satisfactorily in that the effect of long range interatomic interactions are taken into account. It seems that no artifice such as introducing various atomistic models to estimate the stress and energy in the core region is necessary. Moreover, as a continuum theory all problems can be reduced to boundary-initial value problems.

The discussion of the dislocation problems in anisotropic solids is not a trivial extension even in its classical frame of reference. Moreover because of the orientational effects the state of stress and elastic energy are affected considerably. Consequently the criteria for failure or the generation of dislocations need new investigations. The *raison d'être* of the present paper stems from these considerations. In Section 2 we present a brief summary of the field equations of the nonlocal elasticity theory. In Section 3 we obtain the solution of the edge dislocation problem leading to stress and energy fields and in Section 4 we specialize these results to the isotropic crystals. In Section 5, some results of computer calculations are presented and maximum stresses that cause a single edge dislocation in several hexagonal crystals (Mg. Apatite, Cd, Zn) are calculated. The distribution of normal and shear stresses along radial line  $r, \theta=0$ , and as a function of the polar angle  $\theta$  for a fixed  $r$  are calculated. Since no stress and energy singularity occur, the maximum stress hypothesis may be used to calculate the theoretical (cohesive) stress. The results are in the accepted range known from the atomic theory.

COPIES FOR	W. A. Section	<input checked="" type="checkbox"/>	<input type="checkbox"/>
ITIS	BLK Section	<input type="checkbox"/>	<input type="checkbox"/>
IDC			
MANAGING			
JUSTIFICATION			
BY			
DISTRIBUTION			
NOTES			

A

## 2. FORMULATION

In previous papers [2,4] we have shown that, under some very general conditions, the solution of elastostatic problems in linear nonlocal elasticity can be reduced to the solution of the classical Navier's equation, however the stress field is calculated by

$$(2.1) \quad t_{kl}(\underline{x}) = \int_V \alpha(\underline{x}' - \underline{x}) \sigma_{kl}(\underline{x}') dv(\underline{x}')$$

where  $\sigma_{kl}$  is given by the classical Hooke's law which for the hexagonal crystals can be arranged into the form, cf. Fig. 1a,

$$(2.2) \quad \begin{bmatrix} \sigma_{11} \\ \sigma_{22} \\ \sigma_{33} \\ \sigma_{23} \\ \sigma_{31} \\ \sigma_{12} \end{bmatrix} = \begin{bmatrix} c_{11} & c_{12} & c_{13} \\ c_{12} & c_{22} & c_{12} \\ c_{13} & c_{12} & c_{11} \\ & & & 2c_{44} \\ & & & & 2c_{55} \\ & & & & & 2c_{44} \end{bmatrix} \begin{bmatrix} e_{11} \\ e_{22} \\ e_{33} \\ e_{23} \\ e_{31} \\ e_{12} \end{bmatrix}$$

Here  $e_{kl}$  is the linear strain tensor given by

$$(2.3) \quad e_{kl} \equiv \frac{1}{2} (u_{k,l} + u_{l,k})$$

where  $u_{k,l} \equiv \partial u_k / \partial x_l$ . Since for the hexagonal crystals  $2c_{55} = c_{11} - c_{13}$ , the number of independent elastic constants are five.

The attenuation function  $\alpha(\underline{x}' - \underline{x})$  suggested in our previous work is of the form

$$(2.4) \quad \alpha = \alpha_0 \exp[-(k_1/a)^2 (\underline{x}' - \underline{x}_\beta)(\underline{x}' - \underline{x}_\beta) - (k_2/a)^2 (\underline{x}' - \underline{x}_2)^2]$$

where  $\beta$  is summed over  $\beta=1$  and  $\beta=3$ . Here  $a$  is the lattice parameter  $k_1$  and  $k_2$  are two constants which govern the range of attenuation of the interatomic attractions. The constant  $\alpha_0$  is determined from the normalization condition on  $\alpha$ :

$$(2.5) \quad \int_V \alpha(\underline{x}' - \underline{x}) dv(\underline{x}') = 1$$

so that

$$(2.6) \quad \alpha_0 = k_1^2 k_2 / \pi^{3/2} a^3 .$$

Now a problem in nonlocal elasticity is reduced to determining the displacement field  $u_k(\underline{x})$  by solving the Navier's equation obtained by combining (2.2) and (2.3) with the Cauchy's equation

$$(2.7) \quad \sigma_{kl,k} = 0 \quad , \quad k, l = 1, 2, 3$$

where as usual repeated indices are summed over (1,2,3). Once  $u_k(\underline{x})$  is determined one can then calculate strain from (2.3) and the stress field  $t_{kl}$  by using (2.2) in (2.1). We now apply this program to solve the problem of the edge dislocations.



### 3. EDGE DISLOCATION

The straight edge dislocation in a hexagonal crystal is possible in the basal plane  $y=\text{const.}$  in the  $x$ -direction Fig. 1a. We vision such a dislocation by cutting a cylinder along a radial plane and pulling lower surface by a constant amount  $b$  (called Burger's vector) relative to the upper surface and welding the two surfaces, Fig. 1b. The solution of this problem in classical elasticity is well-known (cf. [1], p. 422). The displacement field  $(u_x, u_y, 0)$  satisfying Navier's equation, is given by

$$(3.1) \quad u_x = \frac{b}{4\pi} \left[ \arctan \left( \frac{u_1 xy}{x^2 - \lambda y^2} \right) + u_2 \ln(q/t) \right],$$

$$u_y = \frac{-b}{4\pi} u_3 \left[ u_4 \ln(qt) - u_5 \arctan \left( \frac{u_6 y^2}{x^2 - u_7 y^2} \right) \right]$$

and  $\sigma_{k\ell}$  by

$$(3.2) \quad \sigma_{xx} = -\frac{Mb}{2\pi} \frac{\sigma_1 x^2 y + \sigma_2 y^3}{x^4 + p_1 x^2 y^2 + p_2 y^4},$$

$$\sigma_{yy} = \frac{Mb}{2\pi} \frac{\sigma_3 x^2 y - \sigma_4 y^3}{x^4 + p_1 x^2 y^2 + p_2 y^4},$$

$$\sigma_{xy} = \frac{Mb}{2\pi} \frac{\sigma_3 x^3 - \sigma_4 xy^2}{x^4 + p_1 x^2 y^2 + p_2 y^4}$$

all other components of  $\sigma_{k\ell}$  and  $u_z$  vanish. Here we used  $(x, y, z)$  for subscripts (1, 2, 3) and set

$$(3.3) \quad \bar{c}_{11} \equiv (c_{11}c_{22})^{1/2},$$

$$M \equiv c_{44}(\bar{c}_{11}+c_{12})\{(\bar{c}_{11}-c_{12})/[c_{22}c_{44}(\bar{c}_{11}+c_{12}+2c_{44})]\}^{1/2},$$

$$\sigma_1 \equiv [(\bar{c}_{11}-c_{12})(\bar{c}_{11}+c_{12}+2c_{44})-\bar{c}_{11}c_{44}]/(c_{22}c_{44}),$$

$$\sigma_2 \equiv c_{11}/c_{22}, \quad \sigma_3 \equiv 1, \quad \sigma_4 \equiv (c_{11}/c_{22})^{1/2},$$

$$p_1 \equiv 2(\bar{c}_{11}/c_{22})+(\bar{c}_{11}+c_{12})(\bar{c}_{11}-c_{12}-2c_{44})/(c_{22}c_{44}),$$

$$p_2 \equiv c_{11}/c_{22},$$

$$\lambda \equiv (c_{11}/c_{22})^{1/4}, \quad \phi \equiv \frac{1}{2} \arccos[(c_{12}^2+2c_{12}c_{44}-\bar{c}_{11}^2)/(2\bar{c}_{11}c_{44})],$$

$$q^2 \equiv x^2+2\lambda\cos\phi xy+\lambda^2y^2, \quad t^2 \equiv x^2-2\lambda\cos\phi xy+\lambda^2y^2,$$

$$u_1 \equiv 2\lambda\sin\phi, \quad u_2 \equiv (\bar{c}_{11}^2-c_{12}^2)/(2\bar{c}_{11}c_{44}\sin 2\phi),$$

$$u_3 \equiv \lambda/(\bar{c}_{11}\sin 2\phi), \quad u_4 \equiv (\bar{c}_{11}-c_{12})\cos\phi,$$

$$u_5 \equiv (\bar{c}_{11}+c_{12})\sin\phi, \quad u_6 \equiv \lambda^2\sin 2\phi, \quad u_7 \equiv \lambda^2\cos 2\phi$$

Introducing the cylindrical coordinates by (Fig. 2),

$$(3.4) \quad x = r \cos\theta, \quad y = r \sin\theta, \quad z = z$$

$$x' = r' \cos\theta', \quad y' = r' \sin\theta', \quad z' = z'$$

$$dv(x') = r' dr' d\theta' dz'$$

we have for the components of  $\sigma_{k\ell}$  in cylindrical coordinates:

$$(3.5) \quad \sigma_{rr} = \frac{\sigma_{xx} + \sigma_{yy}}{2} + \frac{\sigma_{xx} - \sigma_{yy}}{2} \cos 2\theta + \sigma_{xy} \sin 2\theta ,$$

$$\sigma_{\theta\theta} = \frac{\sigma_{xx} + \sigma_{yy}}{2} - \frac{\sigma_{xx} - \sigma_{yy}}{2} \cos 2\theta - \sigma_{xy} \sin 2\theta ,$$

$$\sigma_{r\theta} = - \frac{\sigma_{xx} - \sigma_{yy}}{2} \sin 2\theta + \sigma_{xy} \cos 2\theta .$$

The physical components  $t^{(k)}(\ell)$  of the stress tensor in the nonlocal theory are given in terms of those of the classical stresses  $\sigma^{(k)}(\ell)$  and shifters  $\delta^k_{k'}$  by

$$(3.6) \quad t^{(k)}(\ell) = \int_V \alpha(\underline{x}' - \underline{x}) \sigma^{(k')}(\ell') \delta^{\ell'}_{\ell} \delta^k_{k'} dv(\underline{x}')$$

cf. [2]. In cylindrical coordinates the shifters have the following values

$$(3.7) \quad \delta^{1'}_1 = \delta^{2'}_2 = \underline{e}_r \cdot \underline{e}'_r = \underline{e}_\theta \cdot \underline{e}'_\theta = \cos(\theta' - \theta) ,$$

$$\delta^{1'}_2 = \underline{e}'_r \cdot \underline{e}_\theta = \sin(\theta' - \theta) , \quad \delta^{1'}_{2'} = \underline{e}_r \cdot \underline{e}'_{\theta'} = -\sin(\theta' - \theta)$$

$$\delta^{3'}_{3'} = \underline{e}_z \cdot \underline{e}'_z = 1 , \quad \delta^k_{k'} = \delta^{k'}_k .$$

Thus the physical components of the stress tensor have the form



$$\begin{aligned}
 (3.8) \quad t_{rr} &= \int_V \alpha(\underline{x}' - \underline{x}) \left[ \frac{\sigma'_{rr} + \sigma'_{\theta\theta}}{2} + \frac{\sigma'_{rr} - \sigma'_{\theta\theta}}{2} \cos(\theta' - \theta) - \sigma'_{r\theta} \sin 2(\theta' - \theta) \right] dv(\underline{x}') , \\
 t_{\theta\theta} &= \int_V \alpha(\underline{x}' - \underline{x}) \left[ \frac{\sigma'_{rr} + \sigma'_{\theta\theta}}{2} - \frac{\sigma'_{rr} - \sigma'_{\theta\theta}}{2} \cos(\theta' - \theta) + \sigma'_{r\theta} \sin 2(\theta' - \theta) \right] dv(\underline{x}') , \\
 t_{r\theta} &= \int_V \alpha(\underline{x}' - \underline{x}) \left[ \frac{\sigma'_{rr} - \sigma'_{\theta\theta}}{2} \sin 2(\theta' - \theta) + \sigma'_{r\theta} \cos 2(\theta' - \theta) \right] dv(\underline{x}') ,
 \end{aligned}$$

where we used the abbreviation  $\sigma'_{ij} = \sigma'_{ij}(\underline{x}')$ . Using the relations

$$(3.9) \quad \frac{\sigma'_{rr} + \sigma'_{\theta\theta}}{2} = \frac{\sigma'_{xx} + \sigma'_{yy}}{2} , \quad \frac{\sigma'_{rr} - \sigma'_{\theta\theta}}{2} = \frac{\sigma'_{xx} - \sigma'_{yy}}{2} \cos 2\theta' + \sigma'_{xy} \sin 2\theta'$$

(3.8) may be written as

$$\begin{aligned}
 (3.10) \quad t_{rr} &= \int_V \alpha(\underline{x}' - \underline{x}) \left[ \frac{\sigma'_{xx} + \sigma'_{yy}}{2} + \frac{\sigma'_{xx} - \sigma'_{yy}}{2} \cos 2\theta + \sigma'_{xy} \sin 2\theta \right] dv(\underline{x}') , \\
 t_{\theta\theta} &= \int_V \alpha(\underline{x}' - \underline{x}) \left[ \frac{\sigma'_{xx} + \sigma'_{yy}}{2} - \frac{\sigma'_{xx} - \sigma'_{yy}}{2} \cos 2\theta - \sigma'_{xy} \sin 2\theta \right] dv(\underline{x}') , \\
 t_{r\theta} &= \int_V \alpha(\underline{x}' - \underline{x}) \left[ -\frac{\sigma'_{xx} - \sigma'_{yy}}{2} \sin 2\theta + \sigma'_{xy} \cos 2\theta \right] dv(\underline{x}') .
 \end{aligned}$$

The attenuation function  $\alpha(\underline{x}' - \underline{x})$  in cylindrical coordinates acquires the form

$$\begin{aligned}
 (3.11) \quad \alpha(\underline{x}' - \underline{x}) &= \pi^{-3/2} (k_1^2 k_2^2 / a^3) \exp[-(k_1^2 / a^2)(z' - z)^2] \\
 &\quad \cdot \exp[-(r^2 / a^2)(k_1^2 \cos^2 \theta + k_2^2 \sin^2 \theta)] \\
 &\quad \cdot \exp[-(k_1^2 / a^2)(r'^2 \cos^2 \theta' - 2rr' \cos \theta \cos \theta') \\
 &\quad \quad - (k_2^2 / a^2)(r'^2 \sin^2 \theta' - 2rr' \sin \theta \sin \theta')] .
 \end{aligned}$$

We now substitute (3.4) into (3.2), the result and (3.11) into (3.10). This, for each of the stress components, leads to a triple integral over the domain  $(0 \leq r' < \infty, 0 \leq \theta' < 2\pi, -\infty < z' < \infty)$ . The integrations over  $r'$  and  $z'$  are tedious but can be carried out, however the integration over  $\theta'$  will have to be done numerically. Leaving the details of these calculations we give the results:

$$(3.12) \quad \{t_{rr}, t_{\theta\theta}, t_{r\theta}\} = \int_0^{2\pi} \{T_{rr}(\theta, \theta'), T_{\theta\theta}(\theta, \theta'), T_{r\theta}(\theta, \theta')\} \cdot f(r, \theta, \theta') d\theta'$$

where

$$(3.13) \quad T_{rr} = -t_o (g_1 + g_2 \cos 2\theta - g_3 \sin 2\theta)$$

$$T_{\theta\theta} = -t_o (g_1 - g_2 \cos 2\theta + g_3 \sin 2\theta)$$

$$T_{r\theta} = t_o (g_2 \sin 2\theta + g_3 \cos 2\theta)$$

$$g_1 = q_1 \cos^2 \theta' \sin \theta' + q_2 \sin^3 \theta' ,$$

$$g_2 = q_3 \cos^2 \theta' \sin \theta' + q_4 \sin^3 \theta' ,$$

$$g_3 = 2(\sigma_3 \cos^3 \theta' - \sigma_4 \cos \theta' \sin^2 \theta') ,$$

$$\begin{aligned}
f(r, \theta, \theta') = & \frac{\kappa}{4\pi^{1/2}} \exp\{-(kr/a)^2 [1+(\kappa^2-1)\sin^2\theta \\
& - \frac{(\cos\theta\cos\theta'+\kappa^2\sin\theta\sin\theta')^2}{1+(\kappa^2-1)\sin^2\theta'}]\} \\
& \cdot \{1+\operatorname{erf}[(kr/a) \frac{\cos\theta\cos\theta'+\kappa^2\sin\theta\sin\theta'}{[1+(\kappa^2-1)\sin^2\theta']^{1/2}}]\} \\
& \cdot (\cos^4\theta'+p_1\sin^2\theta'\cos^2\theta'+p_2\sin^4\theta')^{-1} [1+(\kappa^2-1)\sin^2\theta']^{-1/2}
\end{aligned}$$

where we also set

$$(3.14) \quad q_1 \equiv \sigma_1 - \sigma_3, \quad q_2 \equiv \sigma_2 + \sigma_4, \quad q_3 \equiv \sigma_1 + \sigma_3, \quad q_4 \equiv \sigma_2 - \sigma_4,$$

$$k_1 \equiv k, \quad k_2/k_1 \equiv \kappa, \quad t_0 \equiv Mb\kappa/2\pi a.$$

The total strain energy is given by

$$(3.15) \quad \Sigma = 2L \int_0^R \int_0^{\pi/2} (t_{rr}e_{rr} + t_{\theta\theta}e_{\theta\theta} + 2t_{r\theta}e_{r\theta}) r \, dr \, d\theta$$

where  $L$  is the length of the cylinder and  $R$  is the radius. Substituting for  $e_{rr}$ ,  $e_{\theta\theta}$  and  $e_{r\theta}$  calculated from (2.3), in the same way as in the case for  $\sigma_{rr}$ ,  $\sigma_{\theta\theta}$ ,  $\sigma_{r\theta}$ , we write

$$\begin{aligned}
(3.16) \quad \Sigma = & \frac{MbL}{\pi} \int_0^R \int_0^{\pi/2} [t_{rr}(a_1\cos^4\theta + a_2\cos^2\theta + a_3)\sin\theta + t_{\theta\theta}(a_4\cos^4\theta \\
& + a_5\cos^2\theta + a_6)\sin\theta + t_{r\theta}(a_7\sin^4\theta + a_8\sin^2\theta + a_9) \\
& \cos\theta] (\cos^4\theta + p_1\sin^2\theta\cos^2\theta + p_2\sin^4\theta)^{-1} d\theta \, dr
\end{aligned}$$

where

$$(3.17) \quad a_1 \equiv (\epsilon_2 - \epsilon_1)(\sigma_1 - \sigma_2) + (\epsilon_2 - \epsilon_3 + \epsilon_4)(\sigma_3 + \sigma_4) ,$$

$$a_2 \equiv -\epsilon_2 \sigma_1 + (2\epsilon_2 - \epsilon_1)\sigma_2 + \epsilon_3 \sigma_3 + (2\epsilon_3 - \epsilon_2 - \epsilon_4)\sigma_4 ,$$

$$a_3 \equiv -(\epsilon_2 \sigma_2 + \epsilon_3 \sigma_4) , \quad a_4 \equiv -a_1 ,$$

$$a_5 \equiv -\epsilon_1 \sigma_1 + (2\epsilon_1 - \epsilon_2)\sigma_2 + \epsilon_2 \sigma_3 + (2\epsilon_2 - \epsilon_3 + \epsilon_4)\sigma_4 ,$$

$$a_6 \equiv -(\epsilon_1 \sigma_2 + \epsilon_2 \sigma_4) , \quad a_7 \equiv 2a_1 ,$$

$$a_8 \equiv 2[(\epsilon_1 - \epsilon_2)\sigma_1 - (\epsilon_2 - \epsilon_3 + \epsilon_4)\sigma_3] - \epsilon_4(\sigma_3 + \sigma_4) ,$$

$$a_9 \equiv \epsilon_4 \sigma_3 ,$$

and

$$(\epsilon_1, \epsilon_2, \epsilon_3) \equiv (c_{22}, -c_{12}, c_{11})(c_{11}c_{22} - c_{12}^2)^{-1} , \quad \epsilon_4 \equiv c_{44}^{-1} .$$

#### 4. ISOTROPIC SOLID

In the case of isotropic solids we have

$$(4.1) \quad M = \mu/(1-\nu) , \quad \kappa=1 , \quad q_1=q_2=2 , \quad q_3=4 , \quad q_4=0 ,$$

$$\sigma_1=3 , \quad \sigma_2=\sigma_3=\sigma_4=1 , \quad p_1=2 , \quad p_2=1 ,$$

$$a_1 = a_2 = a_4 = a_5 = a_7 = a_8 = 0 ,$$

$$a_3 = a_6 = -[2(\lambda + \mu)]^{-1} , \quad a_9 = 1/\mu .$$

Using these values in the expressions of (3.12), (3.13), (3.15) and (3.16) we obtain

$$(4.2) \quad t_{rr} = - \frac{\mu b k}{2\pi(1-\nu)a} \{1 - [1 - \exp(-p^2)]p^{-2}\} p^{-1} \sin\theta ,$$

$$t_{\theta\theta} = \frac{\mu b k}{2\pi(1-\nu)a} \{1 - (2 + p^{-2})[1 - \exp(-p^2)]\} p^{-1} \sin\theta ,$$

$$t_{r\theta} = \frac{\mu b k}{2\pi(1-\nu)a} \{1 - [1 - \exp(-p^2)]p^{-2}\} p^{-1} \cos\theta ,$$

$$(4.3) \quad \Sigma = \frac{\mu b^2 L}{16\pi(1-\nu)^2} \{2(1-\nu)[C + \ln p^2 + E_1(p^2)] - 1 + [1 - \exp(-p^2)]p^{-2}\} ,$$

where  $C$  is the Euler's constant and

$$(4.4) \quad p \equiv kr/a , \quad E_1(x) \equiv \int_x^\infty \frac{e^{-t}}{t} dt , \quad C = 0.5772... .$$

These results are in complete agreement with those given in [3].

## 5. DISCUSSION

Components of the stress tensor are plotted in Fig. 3 as a function of the polar angle  $\theta$  for a fixed radial distance. It is observed that  $t_{rr}$  and  $t_{\theta\theta}$  have the same shape with their extrema occurring at the same angle. The extremum values of  $t_{r\theta}$  differ by an angle  $\pi/2$  from those of the normal stresses. For the fracture calculations the state of stress at  $\theta=0$  and  $\pi/2$  are important. It is known that the cleavage stress



of the crystals is at least twice the maximum shear stress (Kelly [7], p. 17). Of the two state of stress investigated it is found that the one at  $\theta=0$  plane is the most important. In Fig. 4 the shear stress is plotted as a function of  $p=kr/a$  for a few hexagonal crystals (Zn, Cd, Apatite, Mg). The elastic constants of these materials listed in Table 1 are taken from ref. [8]. The shear stress for an isotropic crystal (with  $\nu=0.3$ ) is also plotted in Fig. 4. The ratio of the shear stress in hexagonal crystals to that of the isotropic solids may be useful from the point of view of technological applications. This is given in Fig. 5 for the same crystals. Finally we give a plot of the elastic energy as a function of the radius of the cylinder, Fig. 6. Of course as the radius of the cylinder  $R$  increases the elastic energy also increases. We note however that no singularity is present either in the stress field or in the energy. The usual singularities present in the classical elasticity solutions however appear when the lattice parameter  $a \rightarrow 0$ . This is the classical continuum limit. In Table 1 we give the material moduli, the maximum shear stress and its radial location. The ratio of the attenuation constants  $\kappa$  is taken, by an analogy to the wave propagation [10, ch. 6], as  $\kappa=2C_{22}/(C_{11}+C_{22})$ . In Table 2 the energy ratio of the hexagonal crystals to the isotropic solids is listed for various radii of the cylindrical specimens. Finally, the maximum value of the ratio  $t_{r\theta}/C_{44}$  may be used to estimate the theoretical shear strength of the crystal. To compute this we need to estimate the attenuation constant  $k$  in  $\alpha(\tilde{x}'-\tilde{x})$ . This function decreases to its one percent value at  $n$  lattice parameter distance if

$$k = 2.146/n .$$

As an example, for zinc we have

$$(kb/a)^{-1} t_{r\theta \max} = 0.197 \cdot 10^{11} \text{ dyn/cm}^2 .$$

If we choose  $b=a$  ([9], p. 516) then

$$t_{r\theta \max}/C_{44} = \frac{0.197 \cdot 10^{11}}{3.96 \cdot 10^{11}} k = 0.050k .$$

The maximum value that Kelly ([7], p. 19) gives

$$t_{r\theta \max}/C_{44} = 0.034 .$$

Thus by comparing we obtain

$$k = 0.034/0.050 = 0.68 , \quad n = 2.146/0.68 = 3.14 .$$

The maximum values of  $t_{r\theta}/C_{44}$  are shown on Table 3 for various hexagonal crystals for  $n=2$ ,  $n=2.5$  and  $n=3.0$ . These results are in the right range as predicted by other methods and atomic considerations. For example, in the atomic theory of crystal lattices it is known that one must take into account the interactions of at least eight closest neighbours to obtain a result consistent with experiments [11, 12]. For hexagonal crystals eighth neighbours corresponds to  $n=2$ .

While clearly there is one parameter (namely  $k$ ) which need be estimated, the range of this parameter can be ascertained from our knowledge in condensed matter. The detail shape of the nonlocal



moduli seems to be less effective so long as it is a candidate to be a distribution. The flexibility in the choice of  $\alpha(\underline{x}' - \underline{x})$  and  $k$  should be considered an asset in the sense that for noncrystalline materials and imperfect crystals the attenuation function can be adjusted for a given material once and for all. Afterward all problems for such a solid are reduced to boundary-value problems.

## REFERENCES

- [1] Hirth, J.P. and Lothe, J. [1968]: Theory of Dislocations, McGraw-Hill.
- [2] Eringen, A.C. [1977]: "Screw Dislocation in Nonlocal Elasticity", J. Phys. D: Appl. Phys., Vol. 10, pp. 671-678.
- [3] Eringen, A.C. [1977]: "Edge Dislocation in Nonlocal Elasticity", Int. J. Engng. Sci., Vol. 15, pp. 177-183.
- [4] Eringen, A.C. and F. Balta [1978]: "Screw Dislocation in Nonlocal Hexagonal Elastic Crystals", scheduled for publication in Crystal Lattice Defects.
- [5] Eringen, A.C. [1972]: "Linear Theory of Nonlocal Elasticity and Dispersion of Plane Waves", Int. J. Engng. Sci., 10, 425-435.
- [6] Eringen, A.C. [1976]: Continuum Physics, Vol. IV, Acad. Press.
- [7] Kelly, A. [1966]: Strong Solids, Oxford.
- [8] Hearmon, R.F.S. [1966, 1969]: "The Elastic Constants of Non-Piezoelectric Crystals", Landolt-Börnstein, Numerical Data and Functional Relationships in Science, ed. by Hellwege, K.H., Vols. III/1 and III/2, Springer-Verlag.
- [9] Dorn, J.E. and Mitchell, J.B., [1965]: "Slip Mechanism in Single Crystals of Hexagonal Close-Packed Phases", High Strength Materials, ed. by Zackay, V.F., Wiley.
- [10] Federov, F.I. [1968]: Elastic Waves in Crystals, Plenum.
- [11] Upadhyaya, J.C. and Verma, M.P. [1973]: "Dispersion Relations in some Hexagonal Metals", J. Phys. F: Metal Phys., Vol. 3, p. 640.
- [12] Bertoni, C.M., et.al. [1975]: "Three Body Forces in hcp Metals", J. Phys. F: Metal Phys. Vol. 5, p. 419.

Table 1. Maximum Shear Stresses

Material	Elastic Constants $\times 10^{11}$ dyn/cm <sup>2</sup>					$\kappa$	$t_{r\theta}/t_o$	$F_m$
	$C_{11}$	$C_{12}$	$C_{13}$	$C_{22}$	$C_{44}$			
Zn	16.5	5.0	3.1	6.2	3.96	0.546	0.217	2.30
Mg	5.93	2.14	2.57	6.15	1.64	1.02	0.398	1.45
Cd	11.4	4.00	3.94	5.08	2.00	0.617	0.237	2.05
Apatite	16.7	6.6	1.31	14.0	6.63	0.912	0.389	1.55
Ice(257K)	1.34	0.53	0.65	1.45	0.313	1.04	0.396	1.45

Table 2. Strain Energy Ratio  $\Sigma/\Sigma_o$ 

Material	$p=kr/a$				
	1.	2.	5.	10.	20.
Isotropic( $\nu=.3$ )	0.747	2.000	4.355	6.265	8.199
Isotropic( $\kappa=1$ $\nu=.3$ )	0.748	2.001	4.354	6.263	8.195
Zn	0.265	0.889	2.751	4.563	6.462
Mg	0.739	1.956	4.204	6.021	7.858
Cd	0.260	0.846	2.456	3.960	5.522
Apatite	0.845	2.338	5.272	7.679	10.121
Ice	0.675	1.777	3.807	5.448	7.107

Table 3. Shear Stress  $t_{r\theta}/C_{44}$ 

Material	n		
	2.0	2.5	3.0
Zn	0.053	0.043	0.036
Mg	0.102	0.082	0.068
Cd	0.071	0.057	0.047
Apatite	0.075	0.060	0.050
Ice	0.112	0.090	0.075

## FIGURE CAPTIONS

Figure 1: (a) Hexagonal crystal  
(b) Straight edge dislocation

Figure 2: Cylindrical coordinates

Figure 3: Stresses in xy plane versus  $\theta$ ,  $p=2.30$ .

Figure 4:  $t_{r\theta}/t_o$  versus  $p$ ,  $\theta=0$ . ( $\nu=0.3$  for isotropic case)

Figure 5:  $t_{r\theta}/t_{r\theta}^o$ , ratio of anisotropic to isotropic shear stress at  $\theta=0$ . ( $\nu=0.3$  for isotropic case)

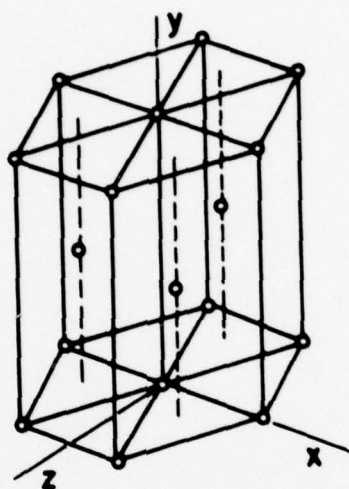
Figure 6:  $\Sigma/Lb^2$  versus  $p=kR/a$

Table 1: Elastic constants and maximum shear stresses

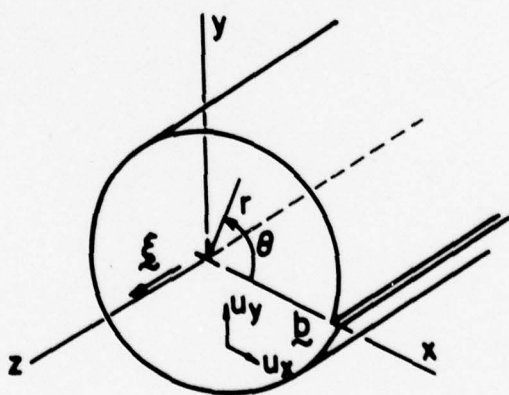
Table 2: Strain energy ratio  $\Sigma/\Sigma_o$

Table 3: Shear stress  $t_{r\theta}/C_{44}$

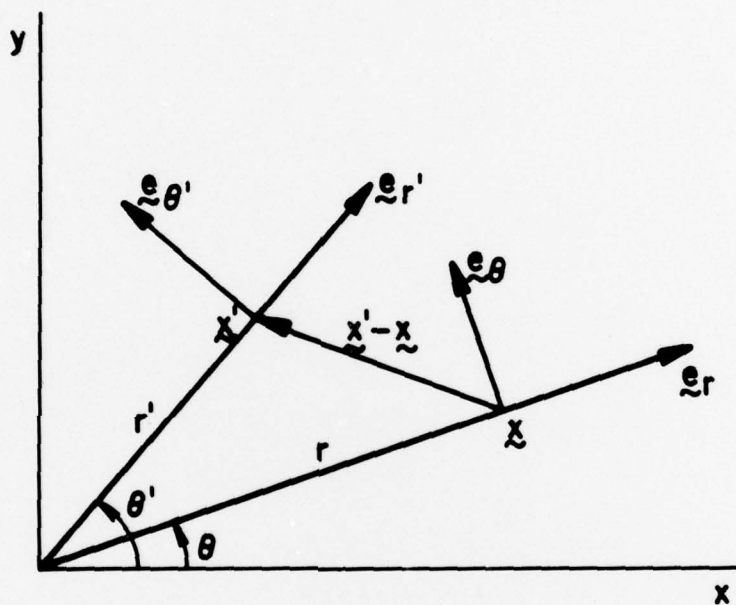




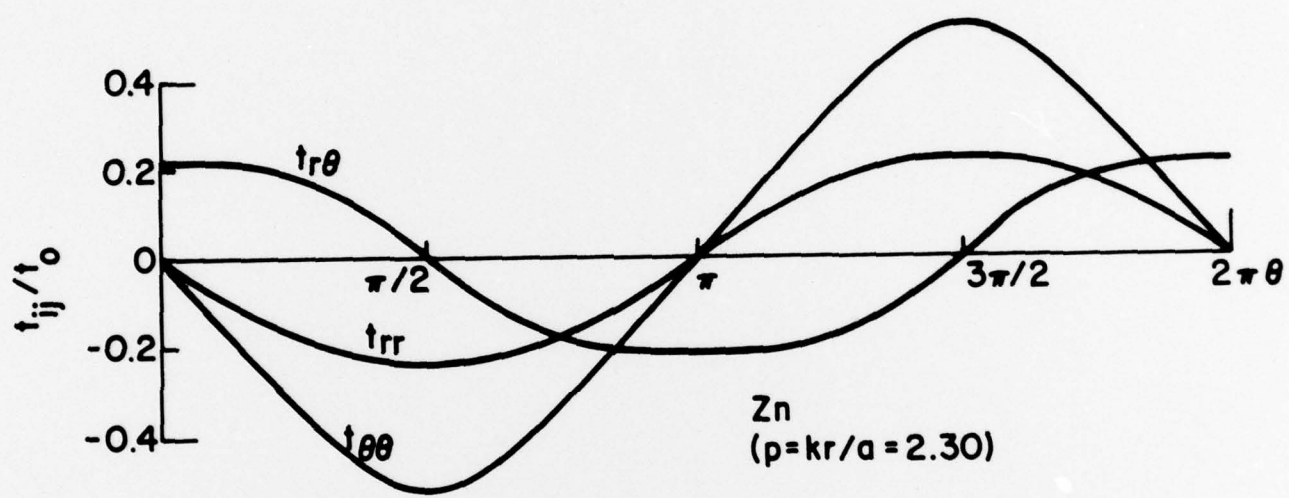
(a)

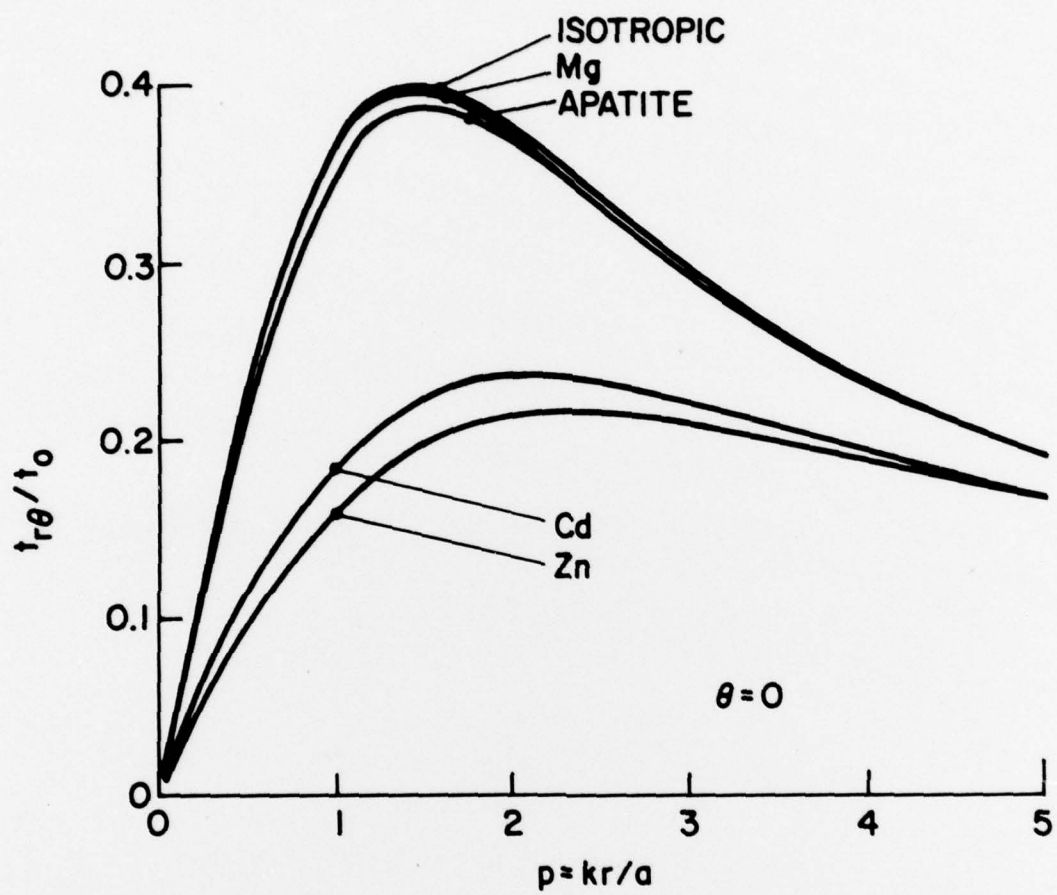


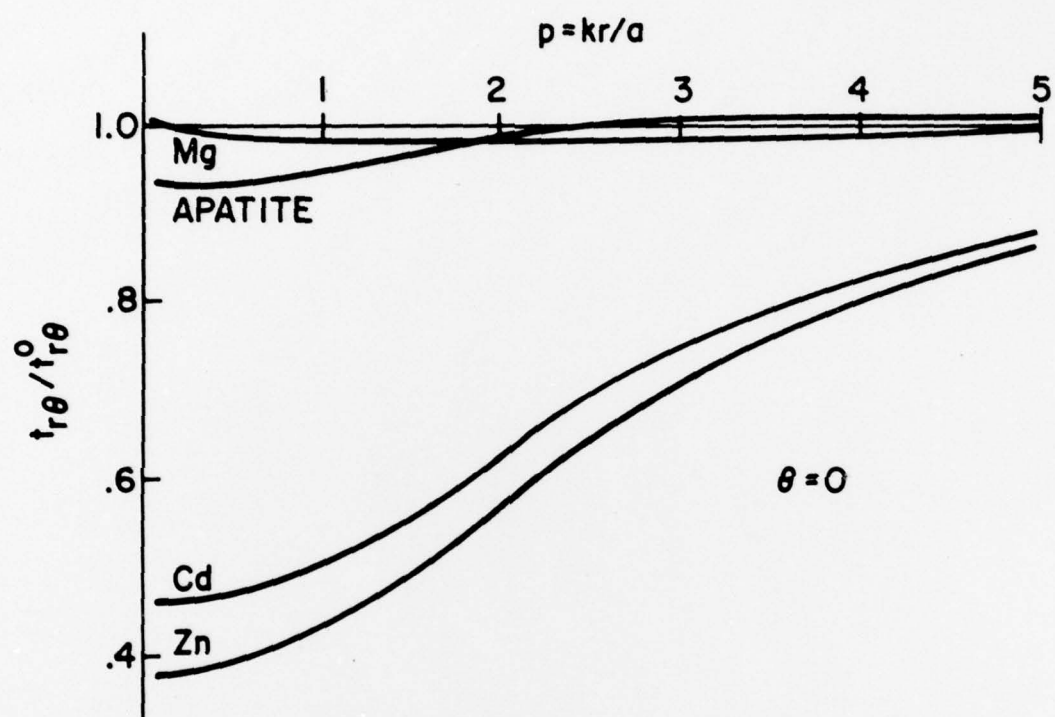
(b)

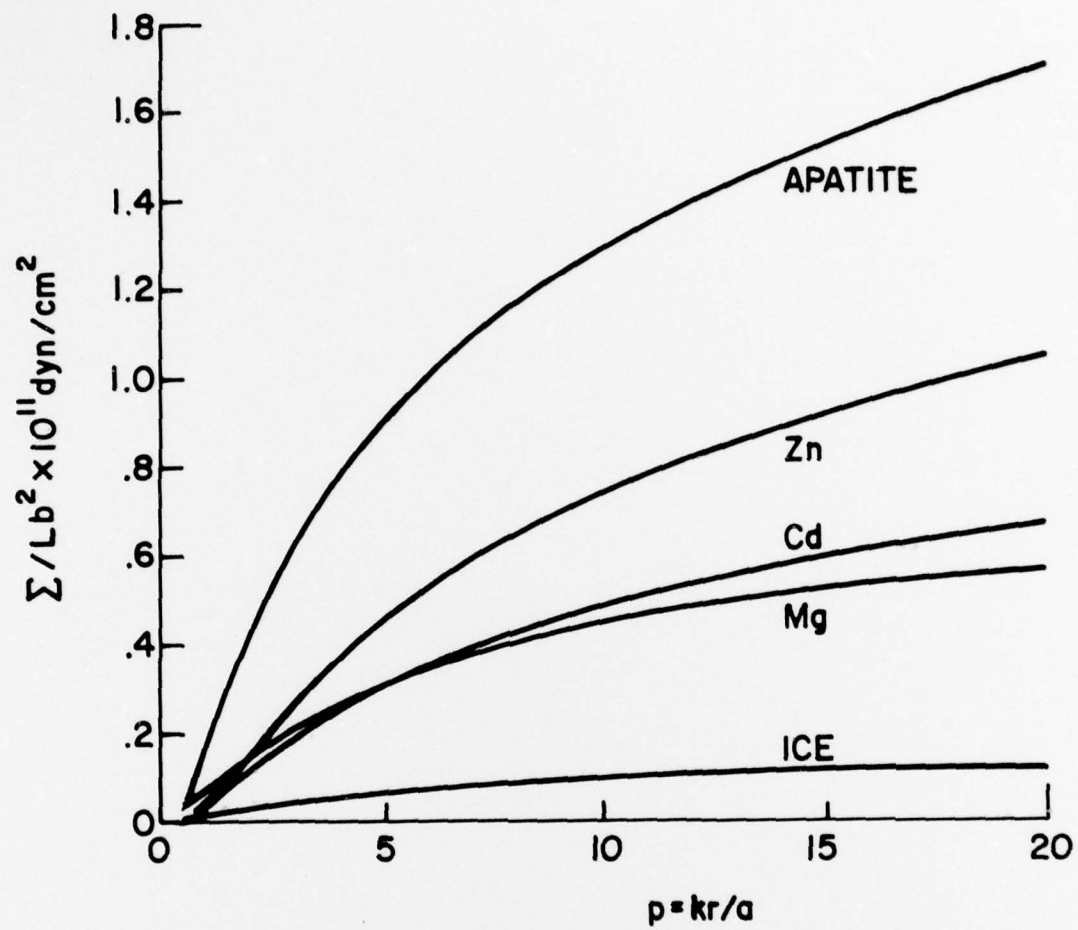












SECURITY CLASSIFICATION OF THIS PAGE (When Data Entered)

REPORT DOCUMENTATION PAGE		READ INSTRUCTIONS BEFORE COMPLETING FORM
1. REPORT NUMBER Technical Report 49 ✓	2. GOVT ACCESSION NO.	3. RECIPIENT'S CATALOG NUMBER
4. TITLE (and Subtitle)  Edge Dislocation in Nonlocal Hexagonal Elastic Crystals		5. TYPE OF REPORT & PERIOD COVERED  Technical Report
		6. PERFORMING ORG. REPORT NUMBER
7. AUTHOR(s)  A. C. Eringen and F. Balta		8. CONTRACT OR GRANT NUMBER(s)  N00014-76-C-0240 ✓
9. PERFORMING ORGANIZATION NAME AND ADDRESS  Princeton University ✓ Princeton, NJ 08540		10. PROGRAM ELEMENT, PROJECT, TASK AREA & WORK UNIT NUMBERS  P00002
11. CONTROLLING OFFICE NAME AND ADDRESS  Office of Naval Research (Code 471) Arlington, VA 22217		12. REPORT DATE May 1978
		13. NUMBER OF PAGES 25
14. MONITORING AGENCY NAME & ADDRESS (if different from Controlling Office)		15. SECURITY CLASS. (of this report)  Unclassified
		15a. DECLASSIFICATION/DOWNGRADING SCHEDULE
16. DISTRIBUTION STATEMENT (of this Report)  Approved for public release; Distribution Unlimited		
17. DISTRIBUTION STATEMENT (of the abstract entered in Block 20, if different from Report)		
18. SUPPLEMENTARY NOTES		
19. KEY WORDS (Continue on reverse side if necessary and identify by block number)  edge dislocation, hexagonal crystals, fracture, nonlocal continuum mechanics		
20. ABSTRACT (Continue on reverse side if necessary and identify by block number) The solution is presented for the problems of edge dislocation in hexagonal crystals with long range interatomic interactions. The field equations of non-local elastic solids are employed to determine the stress fields and the elastic energy for an edge dislocation in the basal plane. Classical stress and energy singularities are found not present in the nonlocal solutions. Stress distribution is calculated and maximum shear stress is given for various hexagonal materials. Theoretical shear stress to initiate a dislocation having a Burger's vector of one atomic distance is calculated and found to be in the		

DD FORM 1 JAN 73 1473

EDITION OF 1 NOV 65 IS OBSOLETE  
S/N 0102-014-6601

SECURITY CLASSIFICATION OF THIS PAGE (When Data Entered)



20. acceptable range known from the lattice dynamic calculations.

**PART 1 - GOVERNMENT**

**Administrative & Liaison Activities**

Chief of Naval Research  
Department of the Navy  
Arlington, Virginia 22217  
Attn: Code 474 (2)  
471  
222

Director  
ONR Branch Office  
495 Summer Street  
Boston, Massachusetts 02210

Director  
ONR Branch Office  
219 S. Dearborn Street  
Chicago, Illinois 60604

Director  
Naval Research Laboratory  
Attn: Code 2629 (ONRL)  
Washington, D.C. 20390 (6)

U.S. Naval Research Laboratory  
Attn: Code 2627  
Washington, D.C. 20390

Director  
ONR - New York Area Office  
715 Broadway - 5th Floor  
New York, N.Y. 10003

Director  
ONR Branch Office  
1030 E. Green Street  
Pasadena, California 91101

Defense Documentation Center  
Cameron Station  
Alexandria, Virginia 22314 (12)

**Army**

Commanding Officer  
U.S. Army Research Office Durham  
Attn: Mr. J. J. Murray  
CRD-AA-IP  
Box CM, Duke Station  
Durham, North Carolina 27706 . 2 .

Commanding Officer  
AMXMR-ATL  
Attn: Mr. R. Shea  
U.S. Army Materials Res. Agency  
Watertown, Massachusetts 02172

Watervliet Arsenal  
MAGGS Research Center  
Watervliet, New York 12189  
Attn: Director of Research

Technical Library

Redstone Scientific Info. Center  
Chief, Document Section  
U.S. Army Missile Command  
Redstone Arsenal, Alabama 35809

Army R&D Center  
Fort Belvoir, Virginia 22060

**Navy**

Commanding Officer and Director  
Naval Ship Research & Development Center  
Bethesda, Maryland 20034

Attn: Code 042 (Tech. Lib. Br.)  
17 (Struc. Mech. Lab.)

172

172

174

177

1800 (Appl. Math. Lab.)

5412S (Dr. W.D. Sette)

19 (Dr. M.M. Sevik)

1901 (Dr. M. Strassberg)

1945

196 (Dr. D. Feit)

1962

Naval Weapons Laboratory  
Dahlgren, Virginia 22448

Naval Research Laboratory  
Washington, D.C. 20375

Attn: Code 8400

8410

8430

8440

6300

6390

6380



Undersea Explosion Research Div.  
Naval Ship R&D Center  
Norfolk Naval Shipyard  
Portsmouth, Virginia 23709  
Attn: Dr. E. Palmer  
Code 780

Naval Ship Research & Development Center  
Annapolis Division  
Annapolis, Maryland 21402  
Attn: Code 2740 - Dr. Y.F. Wang  
28 - Mr. R.J. Wolfe  
281 - Mr. R.B. Niederberger  
2814 - Dr. H. Vanderveldt

Technical Library  
Naval Underwater Weapons Center  
Pasadena Annex  
3202 E. Foothill Blvd.  
Pasadena, California 91107

U.S. Naval Weapons Center  
China Lake, California 93557  
Attn: Code 4062 - Mr. W. Werback  
4520 - Mr. Ken Bischel

Commanding Officer  
U.S. Naval Civil Engr. Lab.  
Code L31  
Port Hueneme, California 93041

Technical Director  
U.S. Naval Ordnance Laboratory  
White Oak  
Silver Spring, Maryland 20910

Technical Director  
Naval Undersea R&D Center  
San Diego, California 92132

Supervisor of Shipbuilding  
U.S. Navy  
Newport News, Virginia 23607

Technical Director  
Mare Island Naval Shipyard  
Vallejo, California 94592

U.S. Navy Underwater Sound Ref. Lab.  
Office of Naval Research  
P.O. Box 8337  
Orlando, Florida 32806

Chief of Naval Operations  
Dept. of the Navy  
Washington, D.C. 20350  
Attn: Code Op07T

Strategic Systems Project Office  
Department of the Navy  
Washington, D.C. 20390  
Attn: NSP-001 Chief Scientist

Deep Submergence Systems  
Naval Ship Systems Command  
Code 39522  
Department of the Navy  
Washington, D.C. 20360

Engineering Dept.  
U.S. Naval Academy  
Annapolis, Maryland 21402

Naval Air Systems Command  
Dept. of the Navy  
Washington, D.C. 20360  
Attn: NAVAIR 5302 Aero & Structures  
5308 Structures  
52031F Materials  
604 Tech. Library  
320B Structures

Director, Aero Mechanics  
Naval Air Development Center  
Johnsville  
Warminster, Pennsylvania 18974

Technical Director  
U.S. Naval Undersea R&D Center  
San Diego, California 92132

Engineering Department  
U.S. Naval Academy  
Annapolis, Maryland 21402

Naval Facilities Engineering Command  
Dept. of the Navy  
Washington, D.C. 20360  
Attn: NAVFAC 03 Research & Development

04 " "  
14114 Tech. Library

Naval Sea Systems Command  
Dept. of the Navy  
Washington, D.C. 20360  
Attn: NAVSHIP 03 Res. & Technology  
031 Ch. Scientist for R  
03412 Hydromechanics  
037 Ship Silencing Div.  
035 Weapons Dynamics

**Naval Ship Engineering Center**

Prince George's Plaza

Hyattsville, Maryland 20782

Attn: NAVSEC 6100 Ship Sys Engr & Des Dep  
6102C Computer-Aided Ship Des  
6105G  
6110 Ship Concept Design  
6120 Hull Div.  
6120D Hull Div.  
6128 Surface Ship Struct.  
6129 Submarine Struct.

**Air Force**

Commander WADD

Wright-Patterson Air Force Base

Dayton, Ohio 45433

Attn: Code WWRMOD

AFFDL (FDDS)

Structures Division

AFLC (MCEEA)

Chief, Applied Mechanics Group  
U.S. Air Force Inst. of Tech.  
Wright-Patterson Air Force Base  
Dayton, Ohio 45433

Chief, Civil Engineering Branch  
WLRC, Research Division  
Air Force Weapons Laboratory  
Kirtland AFB, New Mexico 87117

Air Force Office of Scientific Research  
1400 Wilson Blvd.  
Arlington, Virginia 22209  
Attn: Mechanics Div.

**NASA**

Structures Research Division  
National Aeronautics & Space Admin.  
Langley Research Center  
Langley Station  
Hampton, Virginia 23365

National Aeronautic & Space Admin.  
Associate Administrator for Advanced  
Research & Technology  
Washington, D.C. 02546

Scientific & Tech. Info. Facility  
NASA Representative (S-AK/DL)  
P.O. Box 5700  
Bethesda, Maryland 20014

**Other Government Activities**

Commandant

Chief, Testing & Development Div.  
U.S. Coast Guard  
1300 E. Street, N.W.  
Washington, D.C. 20226

Technical Director  
Marine Corps Dev. & Educ. Command  
Quantico, Virginia 22134

Director

National Bureau of Standards  
Washington, D.C. 20234

Attn: Mr. B.L. Wilson, EM 219

Dr. M. Gaus

National Science Foundation  
Engineering Division  
Washington, D.C. 20550

Science & Tech. Division  
Library of Congress  
Washington, D.C. 20540

Director

Defense Nuclear Agency  
Washington, D.C. 20305  
Attn: SPSS

Commander Field Command  
Defense Nuclear Agency  
Sandia Base  
Albuquerque, New Mexico 87115

Director Defense Research & Engrg  
Technical Library  
Room 3C-128  
The Pentagon  
Washington, D.C. 20301

Chief, Airframe & Equipment Branch  
FS-120  
Office of Flight Standards  
Federal Aviation Agency  
Washington, D.C. 20553

Chief, Research and Development  
Maritime Administration  
Washington, D.C. 20235

Deputy Chief, Office of Ship Constr.  
Maritime Administration  
Washington, D.C. 20235  
Attn: Mr. U.L. Russo

Atomic Energy Commission  
Div. of Reactor Devel. & Tech.  
Germantown, Maryland 20767

Ship Hull Research Committee  
National Research Council  
National Academy of Sciences  
2101 Constitution Avenue  
Washington, D.C. 20418  
Attn: Mr. A.R. Lytle

PART 2 - CONTRACTORS AND OTHER  
TECHNICAL COLLABORATORS

Universities

Dr. J. Tinsley Oden  
University of Texas at Austin  
345 Eng. Science Bldg.  
Austin, Texas 78712

Prof. Julius Miklowitz  
California Institute of Technology  
Div. of Engineering & Applied Sciences  
Pasadena, California 91109

Dr. Harold Liebowitz, Dean  
School of Engr. & Applied Science  
George Washington University  
725 - 23rd St., N.W.  
Washington, D.C. 20006

Prof. Eli Sternberg  
California Institute of Technology  
Div. of Engr. & Applied Sciences  
Pasadena, California 91109

Prof. Paul M. Naghdi  
University of California  
Div. of Applied Mechanics  
Etcheverry Hall  
Berkeley, California 94720

Professor P. S. Symonds  
Brown University  
Division of Engineering  
Providence, R.I. 02912

Prof. A. J. Durelli  
The Catholic University of America  
Civil/Mechanical Engineering  
Washington, D.C. 20017

Prof. R.B. Testa  
Columbia University  
Dept. of Civil Engineering  
S.W. Mudd Bldg.  
New York, N.Y. 10027

Prof. H. H. Bleich  
Columbia University  
Dept. of Civil Engineering  
Amsterdam & 120th St.  
New York, N.Y. 10027

Prof. F.L. DiMaggio  
Columbia University  
Dept. of Civil Engineering  
616 Mudd Building  
New York, N.Y. 10027

Prof. A.M. Freudenthal  
George Washington University  
School of Engineering &  
Applied Science  
Washington, D.C. 20006

D. C. Evans  
University of Utah  
Computer Science Division  
Salt Lake City, Wash 84112

Prof. Norman Jones  
Massachusetts Inst. of Technology  
Dept. of Naval Architecture &  
Marine Engrng  
Cambridge, Massachusetts 02139

Professor Albert I. King  
Biomechanics Research Center  
Wayne State University  
Detroit, Michigan 48202

Dr. V. R. Hodgson  
Wayne State University  
School of Medicine  
Detroit, Michigan 48202

Dean B. A. Boley  
Northwestern University  
Technological Institute  
2145 Sheridan Road  
Evanston, Illinois 60201



Prof. P.G. Hodge, Jr.  
University of Minnesota  
Dept. of Aerospace Engng & Mechanics  
Minneapolis, Minnesota 55455

Dr. D.C. Drucker  
University of Illinois  
Dean of Engineering  
Urbana, Illinois 61801

Prof. N.M. Newmark  
University of Illinois  
Dept. of Civil Engineering  
Urbana, Illinois 61801

Prof. E. Reissner  
University of California, San Diego  
Dept. of Applied Mechanics  
La Jolla, California 92037

Prof. William A. Nash  
University of Massachusetts  
Dept. of Mechanics & Aerospace Engng.  
Amherst, Massachusetts 01002

Library (Code 0384)  
U.S. Naval Postgraduate School  
Monterey, California 93940

Prof. Arnold Allentuch  
Newark College of Engineering  
Dept. of Mechanical Engineering  
323 High Street  
Newark, New Jersey 07102

Dr. George Herrmann  
Stanford University  
Dept. of Applied Mechanics  
Stanford, California 94305

Prof. J. D. Achenbach  
Northwestern University  
Dept. of Civil Engineering  
Evanston, Illinois 60201

Director, Applied Research Lab.  
Pennsylvania State University  
P. O. Box 30  
State College, Pennsylvania 16801

Prof. Eugen J. Skudrzyk  
Pennsylvania State University  
Applied Research Laboratory  
Dept. of Physics - P.O. Box 30  
State College, Pennsylvania 16801

Prof. J. Kempner  
Polytechnic Institute of Brooklyn  
Dept. of Aero. Engrg. & Applied Mech  
333 Jay Street  
Brooklyn, N.Y. 11201

Prof. J. Klosner  
Polytechnic Institute of Brooklyn  
Dept. of Aerospace & Appl. Mech.  
333 Jay Street  
Brooklyn, N.Y. 11201

Prof. R.A. Schapery  
Texas A&M University  
Dept. of Civil Engineering  
College Station, Texas 77840

Prof. W.D. Pilkey  
University of Virginia  
Dept. of Aerospace Engineering  
Charlottesville, Virginia 22903

Dr. H.G. Schaeffer  
University of Maryland  
Aerospace Engineering Dept.  
College Park, Maryland 20742

Prof. K.D. Willmert  
Clarkson College of Technology  
Dept. of Mechanical Engineering  
Potsdam, N.Y. 13676

Dr. J.A. Stricklin  
Texas A&M University  
Aerospace Engineering Dept.  
College Station, Texas 77843

Dr. L.A. Schmit  
University of California, LA  
School of Engineering & Applied Science  
Los Angeles, California 90024

Dr. H.A. Kamel  
The University of Arizona  
Aerospace & Mech. Engineering Dept.  
Tucson, Arizona 85721

Dr. B.S. Berger  
University of Maryland  
Dept. of Mechanical Engineering  
College Park, Maryland 20742

Prof. G. R. Irwin  
Dept. of Mechanical Engrg.  
University of Maryland  
College Park, Maryland 20742

Dr. S.J. Fenves  
Carnegie-Mellon University  
Dept. of Civil Engineering  
Schenley Park  
Pittsburgh, Pennsylvania 15213

Dr. Ronald L. Huston  
Dept. of Engineering Analysis  
Mail Box 112  
University of Cincinnati  
Cincinnati, Ohio 45221

Prof. George Sih  
Dept. of Mechanics  
Lehigh University  
Bethlehem, Pennsylvania 18015

Prof. A.S. Kobayashi  
University of Washington  
Dept. of Mechanical Engineering  
Seattle, Washington 98105

Librarian  
Webb Institute of Naval Architecture  
Crescent Beach Road, Glen Cove  
Long Island, New York 11542

Prof. Daniel Frederick  
Virginia Polytechnic Institute  
Dept. of Engineering Mechanics  
Blacksburg, Virginia 24061

Prof. A.C. Eringen  
Dept. of Aerospace & Mech. Sciences  
Princeton University  
Princeton, New Jersey 08540

Dr. S.L. Koh  
School of Aero., Astro. & Engr. Sc.  
Purdue University  
Lafayette, Indiana 47907

Prof. E.H. Lee  
Div. of Engrg. Mechanics  
Stanford University  
Stanford, California 94305

Prof. R.D. Mindlin  
Dept. of Civil Engrg.  
Columbia University  
S.W. Mudd Building  
New York, N.Y. 10027

Prof. S.B. Dong  
University of California  
Dept. of Mechanics  
Los Angeles, California 90024  
Prof. Burt Paul  
University of Pennsylvania  
Towne School of Civil & Mech. Engrg.  
Rm. 113 - Towne Building  
220 S. 33rd Street  
Philadelphia, Pennsylvania 19104  
Prof. H.W. Liu  
Dept. of Chemical Engr. & Metal.  
Syracuse University  
Syracuse, N.Y. 13210

Prof. S. Bodner  
Technion R&D Foundation  
Haifa, Israel

Prof. R.J.H. Bollard  
Chairman, Aeronautical Engr. Dept.  
207 Guggenheim Hall  
University of Washington  
Seattle, Washington 98105

Prof. G.S. Heller  
Division of Engineering  
Brown University  
Providence, Rhode Island 02912

Prof. Werner Goldsmith  
Dept. of Mechanical Engineering  
Div. of Applied Mechanics  
University of California  
Berkeley, California 94720

Prof. J.R. Rice  
Division of Engineering  
Brown University  
Providence, Rhode Island 02912

Prof. R.S. Rivlin  
Center for the Application of Mathematics  
Lehigh University  
Bethlehem, Pennsylvania 18015

Library (Code 0384)  
U.S. Naval Postgraduate School  
Monterey, California 93940

Dr. Francis Cozzarelli  
Div. of Interdisciplinary  
Studies & Research  
School of Engineering  
State University of New York  
Buffalo, N.Y. 14214



### Industry and Research Institutes

Library Services Department  
Report Section Bldg. 14-14  
Argonne National Laboratory  
9700 S. Cass Avenue  
Argonne, Illinois 60440

Dr. M. C. Junger  
Cambridge Acoustical Associates  
129 Mount Auburn St.  
Cambridge, Massachusetts 02138

Dr. L.H. Chen  
General Dynamics Corporation  
Electric Boat Division  
Groton, Connecticut 06340

Dr. J.E. Greenspon  
J.G. Engineering Research Associates  
3831 Menlo Drive  
Baltimore, Maryland 21215

Dr. S. Batdorf  
The Aerospace Corp.  
P.O. Box 92957  
Los Angeles, California 90009

Dr. K.C. Park  
Lockheed Palo Alto Research Laboratory  
Dept. 5233, Bldg. 205  
3251 Hanover Street  
Palo Alto, CA 94304

Library  
Newport News Shipbuilding &  
Dry Dock Company  
Newport News, Virginia 23607

Dr. W.F. Bozich  
McDonnell Douglas Corporation  
5301 Bolsa Ave.  
Huntington Beach, CA 92647

Dr. H.N. Abramson  
Southwest Research Institute  
Technical Vice President  
Mechanical Sciences  
P.O. Drawer 28510  
San Antonio, Texas 78284

Dr. R.C. DeHart  
Southwest Research Institute  
Dept. of Structural Research  
P.O. Drawer 28510  
San Antonio, Texas 78284

Dr. M.L. Baron  
Weidinger Associates,  
Consulting Engineers  
110 East 59th Street  
New York, N.Y. 10022

Dr. W.A. von Rieseemann  
Sandia Laboratories  
Sandia Base  
Albuquerque, New Mexico 87115

Dr. T.L. Geers  
Lockheed Missiles & Space Co.  
Palo Alto Research Laboratory  
3251 Hanover Street  
Palo Alto, California 94304

Dr. J.L. Tocher  
Boeing Computer Services, Inc.  
P.O. Box 24346  
Seattle, Washington 98124

Mr. William Caywood  
Code BBE, Applied Physics Laboratory  
8621 Georgia Avenue  
Silver Spring, Maryland 20034

Mr. P.C. Durup  
Lockheed-California Company  
Aeromechanics Dept., 74-43  
Burbank, California 91503